

Article

Accuracy of 3D-Printed Occlusal Devices of Different Volumes Using a Digital Light Processing Printer

Sven Reich ^{*}, Saskia Berndt, Christina Kühne  and Hannah Herstell

Department of Prosthodontics and Biomaterials, RWTH Aachen University Hospital, 52074 Aachen, Germany; saskia.berndt@rwth-aachen.de (S.B.); chkuehne@ukaachen.de (C.K.); hannah.herstell@rwth-aachen.de (H.H.)

* Correspondence: sreich@ukaachen.de

Abstract: (1) Background: This in-vitro study was designed to investigate the accuracy of CAD/CAM fabricated occlusal devices with different heights and volumes. (2) Methods: Based on an intraoral scan, an occlusal device with a vertical bite elevation of 2.5 mm and 4.5 mm was digitally designed and 3D printed 10 times. The fabricated occlusal devices were digitized by an industrial structured light scanner (ILS) and provided in stl-format as test objects. The test objects were superimposed with the design dataset as reference to evaluate the accuracy of complete surfaces ([2.5_TOTAL] and [4.5_TOTAL]) with respect to their internal surfaces ([2.5_INTERNAL] and [4.5_INTERNAL]). The mean trueness and precision were calculated based on absolute mean deviation. Absolute and relative volume differences between reference and test were computed. Statistical significances were analyzed performing the Wilcoxon test ($\alpha = 0.05$). (3) Results: As absolute mean deviation trueness values were obtained: $59 \pm 5 \mu\text{m}$ for [2.5_INTERNAL], $98 \pm 9 \mu\text{m}$ for [4.5_INTERNAL], $68 \pm 1 \mu\text{m}$ for [2.5_TOTAL] and $90 \pm 10 \mu\text{m}$ for [4.5_TOTAL]. The precision applying absolute mean deviation was $14 \pm 8 \mu\text{m}$ for [2.5_INTERNAL], $22 \pm 11 \mu\text{m}$ for [4.5_INTERNAL], $19 \pm 10 \mu\text{m}$ for [2.5_TOTAL] and $26 \pm 13 \mu\text{m}$ for [4.5_TOTAL]. The mean trueness and precision values differed significantly. Volume differences of 2.11% for [4.5_TOTAL] and of 2.35% for [2.5_TOTAL] in comparison to their reference file were evaluated. (4) Conclusions: Printed occlusal devices with minor height and volume were more accurate. Both types of devices exhibited results that were comparable to the literature.

Keywords: additive manufacturing; digital light processing; dental; occlusal devices; 3D-printing; accuracy; trueness; precision; intraoral scan (IOS)



Citation: Reich, S.; Berndt, S.; Kühne, C.; Herstell, H. Accuracy of 3D-Printed Occlusal Devices of Different Volumes Using a Digital Light Processing Printer. *Appl. Sci.* **2022**, *12*, 1576. <https://doi.org/10.3390/app12031576>

Academic Editor: Yong-Deok Kim

Received: 31 December 2021

Accepted: 27 January 2022

Published: 1 February 2022

Publisher's Note: MDPI stays neutral with regard to jurisdictional claims in published maps and institutional affiliations.



Copyright: © 2022 by the authors. Licensee MDPI, Basel, Switzerland. This article is an open access article distributed under the terms and conditions of the Creative Commons Attribution (CC BY) license (<https://creativecommons.org/licenses/by/4.0/>).

1. Introduction

Occlusal devices are an important evidence-based therapy option in patients diagnosed with temporomandibular dysfunction [1]. Arthralgia of the temporomandibular joints, myalgia of the temporomandibular muscles or bruxism with parafunctional tooth grinding, gnashing, or clenching are common indications [2–5]. Occlusal devices aim to protect the teeth and restorations from excessive occlusal forces and trauma including the possible reduction of tooth wear [5–8]. Another indication is testing a new vertical occlusal dimension prior to extensive prosthetic rehabilitation [9]. To fabricate conventional occlusal devices, a physical cast is essential. Depending on the type of occlusal device, vacuum thermoforming, sprinkling, or injection molding are commonly used methods to produce occlusal devices from auto-, heat-, or light-polymerized acrylic materials [10–15]. To produce conventional therapeutic devices a technician needs to be involved and many time-consuming working steps are necessary.

As an alternative, computer-aided design/computer-aided manufacturing (CAD/CAM) can be approached [15]. Within the digital workflow, data acquisition is the first step [10,16,17]. For that purpose, intraoral scans or extraoral scans of conventional gypsum casts are necessary [10,16,18]. Based on the obtained virtual casts an occlusal device is designed using a computer aided design software (CAD) [16,17]. Then, this virtual plan

is translated into reality by computer aided manufacturing (CAM) [16,17]. CAM can be distinguished into subtractive and additive manufacturing techniques [16–18]. Both technologies allow unlimited reproduction of the occlusal device based on the existing data in case of damage, fracture, loss or if therapeutic needs require an adjustment of the design [16,19]. In subtractive processes, objects are milled out from prefabricated acrylic resin blocks resulting in high material waste and wear of the milling burs [16]. Additionally, from one blank only a very limited number of pieces can be milled. This results in high time-consumption for manufacturing [17]. On the other hand, volume changes such as shrinkage can be prevented due to the prefabrication of the used materials [20]. In contrast, 3D-printing shows less material waste, a greater degree of freedom due to additive fabrication layer-by-layer from a sliced STL file, and the possibility to print multiple objects simultaneously [21–23].

Additive manufacturing comes with a variety of technologies to process materials in order to build 3D parts. Producing occlusal devices, stereolithography (SLA) and digital light processing (DLP) are mainly used [17–19]. SLA and DLP polymerize photosensitive resins with light. DLP cures one layer of resin at a time using a light source, as for example light-emitting diodes, with wavelength ranges from deep ultraviolet to visible [24,25]. SLA polymerizes one layer point by point with UV light or laser [24–27]. Next to SLA and DLP, continuous liquid interface production (CLIP) is categorized as vat polymerization technology. CLIP is characterized by an oxygen-permeable membrane to inhibit radical polymerization at the surface close to the UV source [24,28]. Hence, it prevents the attachment of a 3D printed object to the oxygen-permeable curing window [29]. Other technologies used in dentistry are fused filament fabrication (FFF) as a material extrusion method, material jetting (MJ), and binder jetting (BJ) technologies as well as powder bed fusion technologies such as selective laser sintering or melting (SLS/M) [28,30]. Fused filament fabrication (FFF) is based on the melting of thermoplastic materials which can then be extruded through a print head or nozzle to form objects by filament layering [31]. For material jetting (MJ) a liquid photosensitive resin is selectively extruded by a print head with hundreds of nozzles and polymerized with UV light [26,32]. Binder Jetting uses the extrusion of a bonding agent through a print head to a powder bed surface. Exposed particles connect through chemical reaction or solvent welding [31]. Selective Laser Sintering and Melting work with a laser to sinter or melt and then fuse powdered materials such as polymers, metal, ceramic or glass, which are applied layer-by-layer via rollers [30,33]. The powder bed is preheated to lower the necessary energy input, and further hinders large thermal differences that can lead to part distortion [31].

Polymers in 3D-printing are composed of monomers, reactive diluents, cross linkers, initiators as well as pigments and fillers [30]. These components affect mechanical properties. Schlotthauer et al. evaluated post-curing depth and homogenous cross-linking depending on varying pigmentation and different UV spectra [34]. Regarding the influence of pigmentation, it was concluded that black pigmentation negatively affected post-curing depth and homogenous cross-linking [34]. A larger wavelength (315–405 nm) resulted in deeper penetration and higher hardness [34]. Another study found that a divergence of the additives' and the resin's reflective index leads to scattering of the laser light resulting in reduced polymerization and inaccuracies [17].

Accuracy is an important factor to assess the usability of printed objects. Various studies investigated the effects of process parameters on three-dimensional accuracy. Parameters as building orientation, post-processing, platform position, layer thickness, laser power and post-curing time were mainly applied to embody the influence on accuracy [22,35,36]. Hui et al. demonstrated that the layer thickness has major effect on accuracy compared to other parameters as laser power, over-cure and scanning distance [22]. Objects built with a low layer thickness and low laser power were the most accurate [22]. Regarding positioning of the 3D objects on the building platform, Unkovski et al. evaluated that the objects arranged on the border of the building platform with a 45° angling resulted in minor deviations [37].

Other important factors influencing overall printing accuracy are polymerization shrinkage, separation stress, and optical image errors [35]. Wu et al. compared the traction stress distribution of tilting and pulling-up separation at different separation speeds [36]. For both separation approaches, the stress increased with separation speed [36]. Moreover, the stress at the external position of the exposure area was greater than at the internal position [36].

Accuracy consists of trueness and precision [38,39]. Trueness is defined as the closeness of agreement between measured test and true reference value [38,39]. To evaluate trueness, deviations between the reference object and its produced replica are calculated [38–40]. Precision is determined as the closeness of agreement between the replicas, generated with the same device and method, to each other [38,39]. Precision includes repeatability and reproducibility [38,39].

The comparison of reference and test object can be executed by 3D surface comparisons or distance measurements [28]. To evaluate the accuracy of printed occlusal devices by superimposition, it is necessary to obtain digital datasets of the fabricated test objects. For digitalization, an industrial structured light scanner is used. High resolution scanners such as ATOS III Triple Scan have a reported trueness of 3 μm and precision of 2 μm [41]. The obtained standard tessellation language (stl) files of the test objects are superimposed with their reference object. As reference object, the virtual design data set of the printed occlusal devices is used. Reference and test objects are aligned via best-fit algorithm and point-to-surface measurements can be performed. Since the registration is performed in a three-dimensional coordinate system, the direction of deviation is demonstrated by negative and positive signs. Values < 0 indicate that the point of the test object is below the reference, values > 0 indicate a supra-position of the test object. The total surface deviation consists of the sum of various point-to-surface measurements. To avoid the compensation of negative and positive values, evaluation with absolute values is required.

According to the definitions of accuracy, a digital light processing (DLP) printer was tested with respect to occlusal devices. The occlusal devices covered the entire arch and two different thicknesses. For surface comparison, the complete surfaces as well as the internal surfaces of the occlusal devices were evaluated. The complete surface was intended to analyze the total deviation, hence the printing process, and its accuracy. By contrast, the internal surface was assessed since it is decisive for the fit and to prevent the inclusion of outliers due to residues of the support structures on the external surface.

The null hypothesis stated was that the occlusal devices did not show statistically significant accuracy with respect to their extension and volume.

2. Materials and Methods

2.1. Design of the Occlusal Device

To create an occlusal device, an existing maxillary and mandibular intraoral scan (Cerec Primescan, software v5.1.3 Dentsply Sirona, Bensheim, Germany) of the study's corresponding author were imported as standard tessellation language (stl) files into a computer-aided design software (inLab SW 22.0 Beta 4, Sirona Dental Systems GmbH, Bensheim, Germany). A computer-aided design application (inLab splint 22.0.1, Sirona Dental Systems GmbH, Bensheim, Germany) was used to design two different types of occlusal devices. At first, the model axis was set, and the insertion axis was defined. Afterwards, the bite splints were designed, and a plane occlusion was chosen. The occlusal vertical dimension was increased by 2.5 mm for the first and by 4.5 mm for the second version of occlusal device. A bilateral canine guidance was added, the spacer was set to 70 μm and a minimal thickness of 1.5 mm was selected.

2.2. Additive Manufacturing

The designs were sent to a computer-aided manufacturing software (inLab CAM software 22.1 Beta 1, Sirona Dental Systems GmbH, Bensheim, Germany) as system-specific cam files. Primeprint (Sirona Dental Systems GmbH, Bensheim, Germany) was selected

as printing device using a specific resin (Primeprint Splint, Sirona Dental Systems GmbH, Bensheim, Germany), with a polymerization wavelength of 385 nm, for additive manufacturing. Default parameters were checked and confirmed including a medium support density, a spherical support tip, and a medium size of the support structures. As orientation strategy “optimized quality” was chosen among “optimized height, footprint and quality”. “Optimized height” results in less printing time since less layers must be polymerized. “Optimized footprint” allows to produce more objects simultaneously than in the case of the option “optimized quality”. In the production options the detail level “very high” was selected which represents a layer thickness of 50 μm . Two devices were positioned automatically and were printed simultaneously. Within one group, each set of devices was positioned identically on the building platform. After printing, the objects were transferred to the post processing unit (Primeprint PPU, Sirona Dental Systems GmbH, Bensheim, Germany) to rinse off resin residues in 99,9% isopropyl alcohol (2-Propanol, VWR International S.A.S., Fontenay-sous-Bois, France) and for additional post-polymerization with ultraviolet light. Finally, the support structures were removed. Based on the designs, with an occlusal vertical dimension increase of 2.5 mm and 4.5 mm, ten samples were printed each. Printing parameters can be found in Table 1.

Table 1. 3D Printing Parameters.

Resin	
Flexural Strength [MPa]	>80
Elastic Modulus [MPa]	>2000
Water Absorption [$\mu\text{g}/\text{mm}^3$]	<32
Solubility [$\mu\text{g}/\text{mm}^3$]	<5
Hardness [Shore D]	>82
Color	clear-transparent
Curing Wavelength [nm]	385
CAM Settings	
Printer	
DMD projector resolution [pixels]	1920 \times 1024
Spectral Maximum of LED	385 nm
Membrane Type of Material Unit	flexible
Support Structures	
Distribution	based on object geometry
Density	Medium
Size	Medium
Spherical Support Tip	Yes
Occlusal Device	
Orientation Strategy	Optimized quality
Detail Level (Layer Thickness [μm])	Very high (50)
Post-Processing	
Washing Solution	99.9% isopropyl alcohol

2.3. Accuracy Evaluation via Surface Comparison

The printed occlusal devices ($n = 10$ (2.5 mm); $n = 10$ (4.5 mm)) were digitized by an industrial structured light scanner (ATOS III Triple Scan, GOM, Topometric GmbH, Göppingen, Germany) to obtain virtual test objects as stl files for accuracy analysis. According to the measuring equipment monitoring protocol the structured light scanner had

a maximum trueness deviation of 4 µm. The precision was ≤ 15 µm. For scanning, the test objects were equipped with reference markers. Internal (Figure 1c) and external surfaces (Figure 1d) of the devices were scanned in two separate measurement series consisting of 20–30 single shots each with varying camera angles. Markers were necessary to match all scans to one three-dimensional data set. The according data sets were referred to as [2.5_TOTAL] and [4.5_TOTAL]. To obtain the reference data in stl format, system specific cam files of the virtually planned 2.5 and 4.5 devices had to be converted. The data of the reference and the test objects were imported in a 3D analysis software (GOM Inspect Suite 2020, GOM GmbH, Braunschweig, Germany) for analysis. The computer-aided design (CAD) stl files were aligned with the corresponding scan stl files of the printed occlusal device ([2.5_TOTAL] and [4.5_TOTAL]) for trueness evaluation. To register two different stl files in one coordinate system both files were superimposed via best-fit alignment. After that, surface comparison was performed (Figure 1e,f). For analysis, two approaches were taken. Next to the total surface [2.5_TOTAL; 4.5_TOTAL] of the occlusal device, the internal surfaces [2.5_INTERNAL; 4.5_INTERNAL] (Figure 1g,h) were evaluated to focus on the fit of the devices on the occlusal surfaces of the teeth. Therefore, the external surface of the devices was cut-off. Before point-to-surface measurement, the maximum tolerance was set to one millimeter and the surface comparison was applied on the test object.

The values of the point-to-surface measurements between two surfaces were exported as absolute values in American Standard Code for Information Interchange (ASCII). A self-programmed python script was used for automated data evaluation. For each file the absolute mean deviation, root mean square error, median, standard deviation, and minimal and maximal distances were calculated. RMSE is defined as:

$$RMSE = \sqrt{\frac{1}{n} \sum_{i=1}^n (x_i - \mu_i)^2}$$

where x_i are the predicted values of the reference cast, μ_i are the observed values of the test cast, and n is the number of observations. The RMSE describes the dispersion around a true value with respect to trueness and precision.

To check precision, each group's scans ($n = 10$: [2.5_TOTAL]; [4.5_TOTAL]; and [4.5_INTERNAL]) were compared among each other resulting in 45 surface comparisons per group. The data analysis was performed as above.

In addition, volumes of each stl file (reference, [2.5_TOTAL], and [4.5_TOTAL]) were calculated in mm³.

2.4. Statistics

SPSS 26 (IBM Corporation, Armonk, NY, USA) was used for statistic calculations.

The Shapiro–Wilk test revealed that the trueness and precision data of [2.5_INTERNAL] and [4.5_INTERNAL] were not normally distributed. Therefore, the Wilcoxon test (Bonferroni corrected) was applied to check whether there was a statistically significant difference between [2.5_INTERNAL] and [4.5_INTERNAL] at $p \leq 0.05$. The trueness data of [4.5_TOTAL] and precision data of [2.5_TOTAL] and [4.5_TOTAL] were not normally distributed according to the Shapiro–Wilk test. [2.5_TOTAL] and [4.5_TOTAL] were tested for significant differences using the Wilcoxon test.

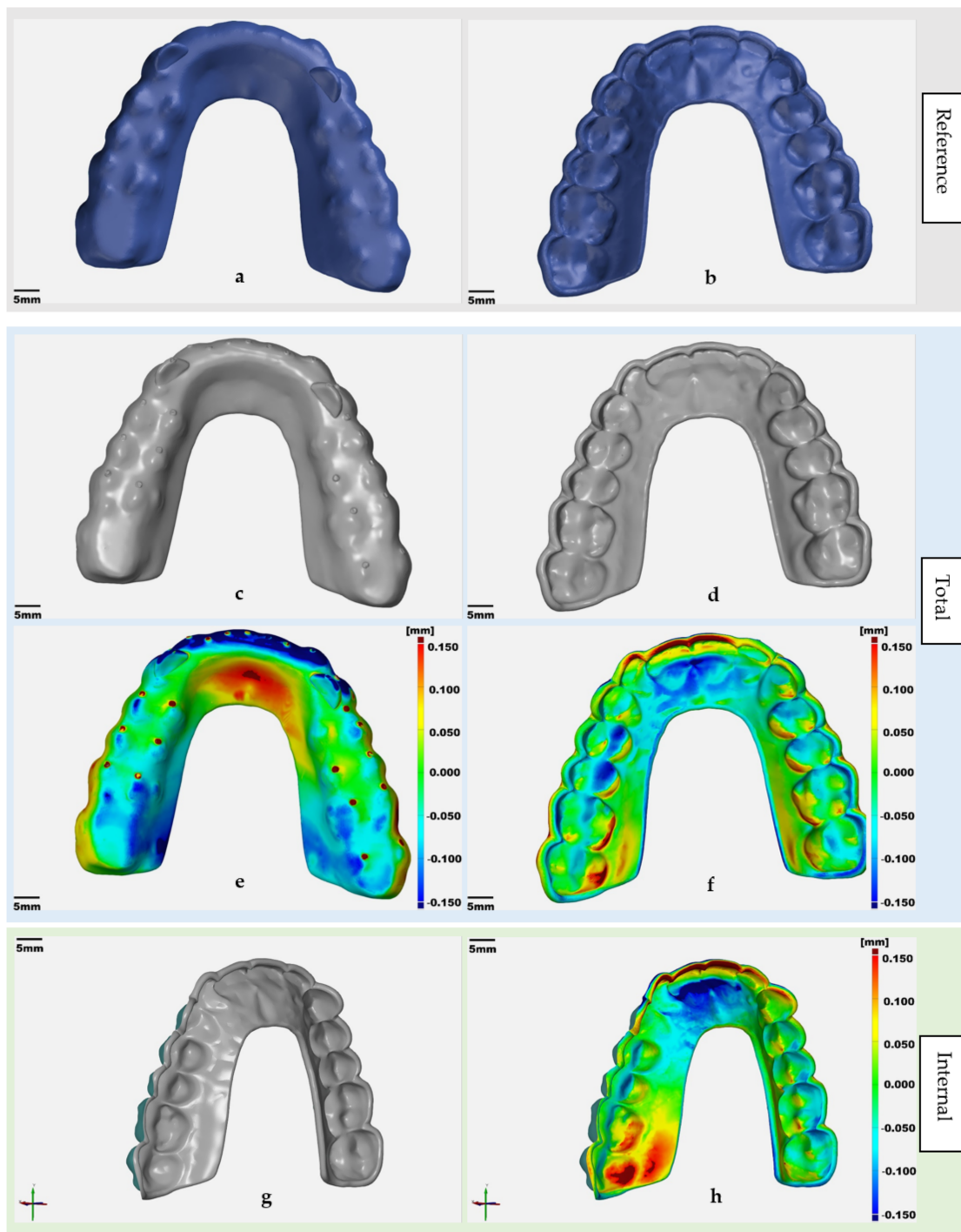


Figure 1. Reference file with (a) external and (b) internal surfaces; test file [TOTAL] with (c) external, (d) internal surfaces and the respective color-coded surface after comparison with the reference file (Scale $\pm 150 \mu\text{m}$) (e,f); (g) test file [INTERNAL] and the respective surface comparison with the reference file (Scale $\pm 150 \mu\text{m}$) (h).

3. Results

3.1. Evaluation of the Internal Surfaces

3.1.1. Trueness

The trueness data of [2.5_INTERNAL] and [4.5_INTERNAL] are displayed in Table 2.

Table 2. Trueness [2.5_INTERNAL] and [4.5_INTERNAL].

	n	Absolute Mean Deviation [μm]				RMS Error [μm]			
		Minimum	Maximum	Mean \pm Standard Deviation	Median	Minimum	Maximum	Mean \pm Standard Deviation	Median
[2.5_INTERNAL]	10	54	64	59 \pm 5	59	70	83	77 \pm 6	77
[4.5_INTERNAL]	10	73	98	80 \pm 9	78	97	130	106 \pm 12	103

The mean trueness was 59 μm (SD \pm 5 μm) for [2.5_INTERNAL] and 80 μm (SD \pm 9 μm) for [4.5_INTERNAL]. The mean trueness values differed significantly.

The mean RMSE was 77 μm (SD \pm 6 μm) for [2.5_INTERNAL] and 106 μm (SD \pm 12 μm) for [4.5_INTERNAL]. The RMSE values differed significantly.

3.1.2. Precision

The precision data of [2.5_INTERNAL] and [4.5_INTERNAL] are displayed in Table 3.

Table 3. Precision [2.5_INTERNAL] and [4.5_INTERNAL].

	n	Precision Based on Absolute Deviation [μm]				Precision Based on RMS Error [μm]			
		Minimum	Maximum	Mean \pm Standard Deviation	Median	Minimum	Maximum	Mean \pm Standard Deviation	Median
[2.5_INTERNAL]	10	3	22	14 \pm 8	20	5	29	19 \pm 10	27
[4.5_INTERNAL]	10	4	40	22 \pm 11	22	8	52	31 \pm 13	29

The precision, applying absolute deviation values, was 14 μm (SD \pm 8 μm) for and 22 μm (SD \pm 11 μm) for [4.5_INTERNAL]. The values differed significantly.

The precision based on RMSE was 19 μm (SD \pm 10 μm) for [2.5_INTERNAL] and 31 μm (SD \pm 13 μm) for [4.5_INTERNAL]. The values differed significantly.

3.2. Evaluation of the Total Surface

3.2.1. Trueness

The trueness data of [2.5_TOTAL] and [4.5_TOTAL] are displayed in Table 4.

Table 4. Trueness [2.5_TOTAL] and [4.5_TOTAL].

	n	Absolute Mean Deviation [μm]				RMS Error [μm]			
		Minimum	Maximum	Mean \pm Standard Deviation	Median	Minimum	Maximum	Mean \pm Standard Deviation	Median
[2.5_TOTAL]	10	65	69	68 \pm 1	68	83	91	88 \pm 3	88
[4.5_TOTAL]	10	82	109	90 \pm 10	87	113	145	122 \pm 12	118

The mean trueness was 68 μm [SD \pm 1 μm] for [2.5_TOTAL] and 90 μm [SD \pm 10 μm] for [4.5_TOTAL]. The mean trueness values differed significantly.

The mean RMSE was 88 μm [SD \pm 3 μm] for [2.5_TOTAL] and 122 μm [SD \pm 12 μm] for [4.5_TOTAL]. The RMSE values differed significantly.

3.2.2. Precision

The precision data of [2.5_TOTAL] and [4.5_TOTAL] are displayed in Table 5.

Table 5. Precision [2.5_TOTAL] and [4.5_TOTAL].

	n	Precision Based on Absolute Deviation [μm]				Precision Based on RMS Error [μm]			
		Minimum	Maximum	Mean \pm Standard Deviation	Median	Minimum	Maximum	Mean \pm Standard Deviation	Median
[2.5_TOTAL]	10	6	29	19 \pm 10	26	21	46	34 \pm 8	37
[4.5_TOTAL]	10	7	45	26 \pm 13	25	23	65	42 \pm 12	41

The mean precision values, applying absolute deviation values, were 19 μm [SD \pm 10 μm] for [2.5_TOTAL] and 26 μm [SD \pm 13 μm] for [4.5_TOTAL]. [2.5_TOTAL] and [4.5_TOTAL] differed significantly.

The mean precision based on RMSE values were 34 μm [SD \pm 8 μm] for and 42 μm [SD \pm 12 μm] for [4.5_TOTAL]. [2.5_TOTAL] and [4.5_TOTAL] differed significantly.

3.3. Evaluation of Volume

Absolute and relative volume differences comparing the mean volume of the printed occlusal devices [2.5_TOTAL] and [4.5_TOTAL] with their corresponding reference CAD file of are shown in Table 6.

Table 6. Absolute and relative volume differences between reference and prints.

[2.5_TOTAL]	Volume [mm^3]
Reference file	5682.69
Printed (mean) (N = 10)	5548.93
Absolute Volume Difference	133.76
Relative Volume Difference	2.35%
[4.5_TOTAL]	Volume [mm^3]
Reference file	6737.55
Printed (mean) (N = 10)	6595.38
Absolute Volume Difference	142.17
Relative Volume Difference	2.11%

4. Discussion

The aim of this study was to test whether there was a statistically significant difference between occlusal devices printed for the same jaw but of different height and volume. The results revealed that the null hypothesis had to be rejected.

The volume measurements showed that there was a minimal shrinkage of the printed object in relation to the reference data file. In relation to their reference files, for the more voluminous [4.5_TOTAL], a volume difference of approximately 2.11% and for of approximately 2.35% was measured. This may lead to the conclusion that the polymerization shrinkage of the resin during printing was not completely compensated.

The comparison of the trueness values of the [2.5_TOTAL] and the [2.5_INTERNAL] and of the [4.5_TOTAL] and the [4.5_INTERNAL] revealed only minor differences. The low precision values of all four data sets [2.5_TOTAL], [2.5_INTERNAL], [4.5_TOTAL], and [4.5_INTERNAL] confirmed a good reproducibility referring to absolute deviations. With respect to precision, the maximum difference between the absolute deviations and the RMSE values was 16 μm . These small differences underline the good reproducibility as RMSE squares all deviations, because the RMSE is more sensitive to outliers.

For [2.5_INTERNAL] the mean trueness was 59 μm (SD \pm 5 μm). Wesemann et al. revealed mean positive deviations around +174 μm [SD \pm 66 μm] and mean negative deviations

around $-135 \mu\text{m}$ [$\text{SD} \pm 60 \mu\text{m}$] using a DLP printer for occlusal devices with a material thickness of 1. mm [42]. In comparison, SLA technology showed mean positive deviations of $+105 \mu\text{m}$ [$\text{SD} \pm 18 \mu\text{m}$] and mean negative deviations of $-85 \mu\text{m}$ [$\text{SD} \pm 15 \mu\text{m}$] [42]. The present study exhibited lower results; [2.5_INTERNAL] showed a mean absolute deviation of $59 \mu\text{m}$, while the DLP printer results described above would lead to mean deviation of $154.5 \mu\text{m}$ $((174 + 135)/2)$. The [4.5_INTERNAL] showed better results with an absolute mean trueness of $80 \mu\text{m}$ as well. The [2.5_INTERNAL] also achieved better trueness in contrast to the SLA printer which exhibited a mean absolute deviation of $95 \mu\text{m}$ $((105 + 85)/2)$.

Reymus et al. evaluated the accuracy of the intaglio surfaces of printed occlusal devices (material thickness: 2 mm) which were horizontally and vertically positioned on the building platform [17]. For horizontal positioning, trueness RMSE values of $71.30 \mu\text{m}$ [$\text{SD} \pm 2.11 \mu\text{m}$] (OrthoClear, NextDent, Soesterberg, The Netherlands), $101.99 \mu\text{m}$ [$\text{SD} \pm 4.79 \mu\text{m}$] (Freeprint Splint, Detax, Ettlingen, Germany) and $77.17 \mu\text{m}$ [$\text{SD} \pm 3.22 \mu\text{m}$] (V-Splint, VOCO, Cuxhaven, Germany) were achieved using different DLP printers [17]. SLA resulted in RMSE values of $76.61 \mu\text{m}$ [$\text{SD} \pm 4.46 \mu\text{m}$] (Dental LT, Formlabs, MA, USA) [17]. The DLP printer investigated in the present study revealed better or similar results and was competitive to the SLA printer.

Reymus et al. also presented precision RMSE values of $31.12 \mu\text{m}$ [$\text{SD} \pm 3.25 \mu\text{m}$] (OrthoClear, D20 II), $41.22 \mu\text{m}$ [$\text{SD} \pm 8.27 \mu\text{m}$] (Freeprint Splint, D20 II), and $58.22 \mu\text{m}$ [$\text{SD} \pm 3.53 \mu\text{m}$] (V-Splint, SolFlex 350) for horizontal positioning. The SLA printer revealed precision RMSE values of $51.80 \mu\text{m}$ [$\text{SD} \pm 8.01 \mu\text{m}$] (Dental LT, Form 2) [17]. The vertical orientation presented RMSE values of $19.42 \mu\text{m}$ [$\text{SD} \pm 2.62 \mu\text{m}$] (OrthoClear, D20 II), $19.47 \mu\text{m}$ [$\text{SD} \pm 2.82 \mu\text{m}$] (Freeprint Splint, D20 II) and $24.40 \mu\text{m}$ [$\text{SD} \pm 2.48 \mu\text{m}$] (V-Splint, SolFlex 350), and $109.20 \mu\text{m}$ [$\text{SD} \pm 13.50 \mu\text{m}$] (Dental LT, Form 2) were described [17]. The study of Reymus et al. revealed that a different orientation of the printed object may lead to different trueness and precision values [17]. In our study, precision RMSE values were $19 \mu\text{m}$ [$\text{SD} \pm 10 \mu\text{m}$] for [2.5_INTERNAL] and $31 \mu\text{m}$ [$\text{SD} \pm 13 \mu\text{m}$] for [4.5_INTERNAL], so that the precision performed was comparable or better.

Studies evaluating the accuracy of CAD/CAM occlusal devices are limited. However, there are remotely comparable investigations focusing on the accuracy of denture bases [42]. Yoon et al. assessed the trueness of the intaglio surfaces of milled (MIL) and printed (DLP) mandibular complete denture bases [43]. They revealed negative and positive mean trueness values of $93 \mu\text{m}$ [$\text{SD} \pm 10 \mu\text{m}$] and $-68 \mu\text{m}$ [$\text{SD} \pm 10 \mu\text{m}$] for DLP and $21 \mu\text{m}$ [$\text{SD} \pm 4 \mu\text{m}$] and $-43 \mu\text{m}$ [$\text{SD} \pm 4 \mu\text{m}$] for MIL. In the present study, the intaglio surfaces showed an absolute mean trueness of $59 \mu\text{m}$ [$\text{SD} \pm 5 \mu\text{m}$] for [2.5_INTERNAL] and of $80 \mu\text{m}$ [$\text{SD} \pm 9 \mu\text{m}$] for [4.5_INTERNAL]. The comparison of the values of the present study with those of Yoon et al. have to be considered very carefully. Although mandibular denture bases have a similar extension to occlusal devices, their intaglio surface is less structured. Different test methods could have been applied in detail. When comparing the results for printed denture bases and printed occlusal devices, the transparency of the respective resin must be addressed [42]. Transparent resins can affect printing resolution due to the absence of absorbing pigments [42]. The depth of cure, determining the z-resolution, is influenced by the photoinitiator, pigments, dyes, or added UV absorbers, as well as exposure conditions such as wavelength, power, and exposure time/velocity [31]. UV absorbers are required when printing transparent materials [31].

Next to material qualities, there are other parameters which might compromise printing results. The orientation on the printer platform, layer thickness, the post-processing method, exposure times, x, y resolution, z resolution, detaching forces and printing technology must be acknowledged [17,45,46]. Thermal expansion or contraction during polymerization can cause dimensional errors, too, since these factors define the degree of polymerization shrinkage [44]. During post-processing additional polymerization using UV light and heat can result in further shrinkage with the occurrence of warping [45,46]. Park et al. analyzed the three-dimensional accuracy within the x, y, and z-axis [45]. Based on their findings, deviations of the z-axis were generally smaller than those in the x- and y-axis [45]. They stated that the z-axis is stationary during material application and moves

to the next layer when printing pauses which they considered as a possible explanation [45]. Furthermore, they concluded that FFF and DLP printed casts tended to contract, whereas Polyjet and SLA groups expanded buccolingually and anterioposteriorly [45]. With respect to the DLP printer this statement could not be confirmed in the present study because [2.5_TOTAL] and [4.5_TOTAL] exhibited contrary deviation patterns.

To visualize shrinkage or other dimensional effects, color-coded deviation images are of major interest. These images allow us to determine recurring deviation patterns. The color-coded deviation images of all ten [2.5_TOTAL] scans show similar dimensional differences between them and their reference file. Looking at the external surface (Figure 2a), the posterior area seems to become wider with a simultaneous compression of the anterior area. A relative decrease of material, in relation to the reference file, is indicated by the color code at the posterior oral side. At the buccal posterior side, a relative increase can be noticed. In the anterior area the labial part of the device exhibits a relative reduction of the front arch and a corresponding addition of the oral area. Analyzing the internal surfaces (Figure 2b), a relative increase of the inner labial anterior area was visible. At the same time, a decrease at the inner oral anterior side was visible. In the posterior area, this phenomenon was exactly the opposite.

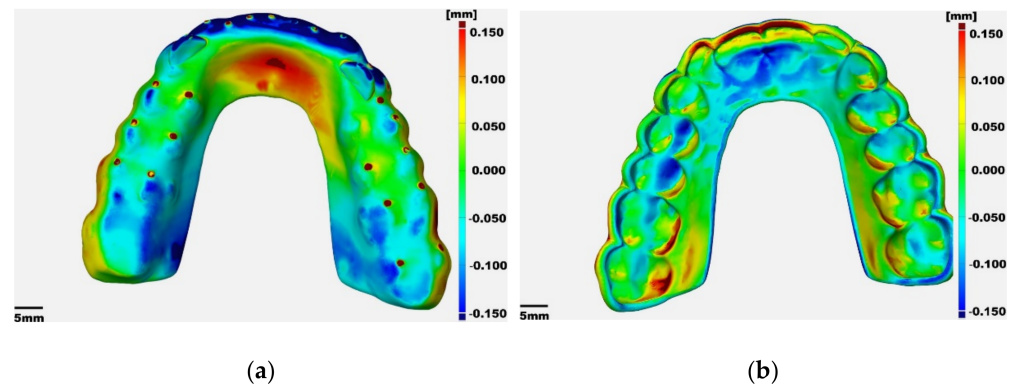


Figure 2. Representative example of the surface deviations of [2.5_TOTAL] (Scale $\pm 150 \mu\text{m}$) from the reference data file with respect to the; (a) external surface; (b) internal surface.

For the [4.5_TOTAL] occlusal devices, a different pattern of increase and decrease of material was observed in comparison to the reference file. Regarding the external surfaces (Figure 3a), the posterior oral side showed a material increase which was more prominent on the left side than on the right side. On the respective internal surfaces (Figure 3b) of the posterior oral side, a corresponding decrease was visible. The posterior buccal area showed a relative increase of material at the inner side and a decrease at the outer side. As a result, the arch of the occlusal device becomes narrower.

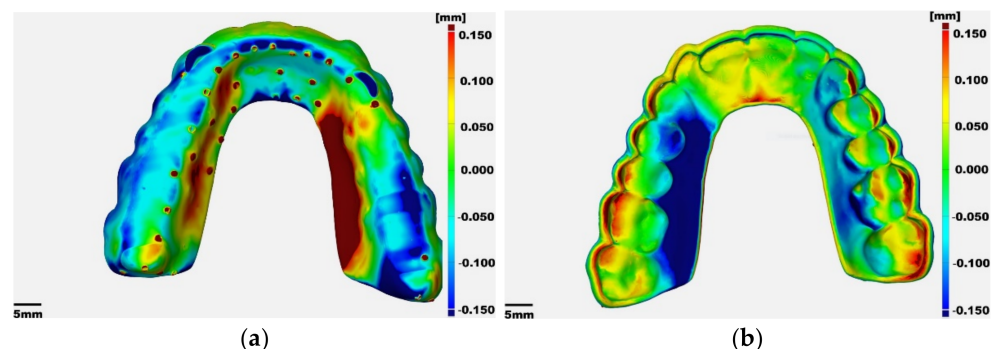


Figure 3. Representative example of the surface deviations of [4.5_TOTAL] (Scale $\pm 150 \mu\text{m}$) from the reference data file with respect to the; (a) external surface; (b) internal surface.

These asymmetrical observations between [2.5_TOTAL] and [4.5_TOTAL] could be explained by the orientation of the object on the building platform (Figure 4). The inclination and tilting influence the draining of the polymer during printing when the platform is vertically moved. The post processing including rinsing and the post polymerization may have been influenced by the position, too. The 2.5 and 4.5 occlusal devices were not identically positioned on the building platform. “Optimized quality” was chosen as orientation strategy. The aim of the “optimized quality” option is that the best possible position of the printed object on the platform is calculated by the CAM software. In this way, uncured polymer residues and unsupported undercuts are avoided, and functional/intaglio surfaces are protected from the placement of support structures. Dependent on the different dimensions the 2.5 and 4.5 samples were positioned differently on the platform by the software when choosing the “optimized quality” option. These observations require further tests by varying the orientation of the occlusal devices on the building platform.

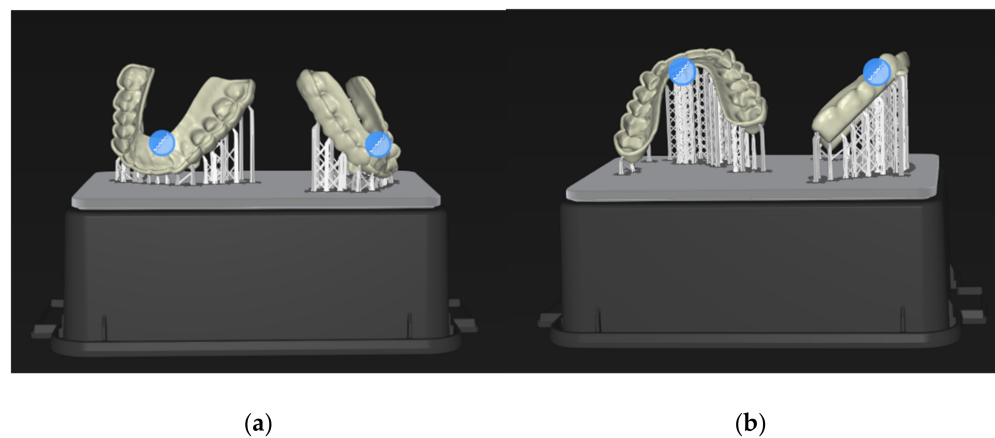


Figure 4. Orientations of the occlusal devices on the building platform (a) 2.5 (b) 4.5.

Of course, the higher volume of the [4.5_TOTAL] compared to [2.5_TOTAL] may have been also a co-factor for higher trueness values. As discussed, the percentage of shrinkage of both devices was similar.

Limitations

Since the support structures were placed on the external surfaces of the devices, some residues were left after removal. These residues are included in the volume calculation (Figure 2a) due to no further processing of the devices. In consequence, the devices' volumes are distorted a bit towards the original volume.

The present study was limited to the comparison of the CAM file with the corresponding printed sample. Of course, this is the correct approach to evaluate the pure deviation between virtual file and physical object. However, for the evaluation of the clinical practicability the entire workflow including impression taking must be investigated.

As mentioned before, the dimensions of an object decisively influence the print parameters such as platform orientation and, in consequence, the print result. In the present study only one situation represented by one single cast and one design were used. More studies investigating a higher variety of shapes would be desirable.

5. Conclusions

In this paper we evaluated the trueness and precision of 3D printed occlusal devices with different height and volumes ([2.5_TOTAL] and [4.5_TOTAL]) obtained from a DLP printer using a transparent resin. The occlusal devices [2.5_TOTAL] were less voluminous than the [4.5_TOTAL]. The applied layer thickness of 50 μm was representative of a high detail level. We can draw the following conclusions from the results:

- The printing and post-processing process were accompanied by a minimal shrinkage. The volume of the printed objects was between 2.11% and 2.35% less in comparison to the CAM files, which served as blueprint;
- Within their groups, the [2.5_TOTAL] and [4.5_TOTAL] devices showed identical dimensional deviations in comparison to their corresponding stl references. However, between the two groups different deviation patterns were observed. The [2.5_TOTAL] were wider in the posterior region and compressed in the anterior area. The [4.5_TOTAL] showed a compression of the posterior area;
- These observations confirmed that deviation patterns are not rigidly associated with the specific printer system but with different parameters. The different platform orientations specified by the CAM software for [2.5_TOTAL] and [4.5_TOTAL] and the different volumes could be identified as such influential variables;
- The results revealed a high precision. The absolute mean deviation values were 19 μm for [2.5_TOTAL] and 26 μm for [4.5_TOTAL]. The high precision was underlined to be the more outlier sensitive RMSE value which revealed 34 μm for [2.5_TOTAL] and 42 μm for [4.5_TOTAL];
- The absolute mean trueness was 68 μm for [2.5_TOTAL] and 90 μm for [4.5_TOTAL]. The median RMSE results were 88 μm for [2.5_TOTAL] and 122 μm for [4.5_TOTAL]. Thus, the results were comparable with previously published printer results;
- There were statistically significant differences between [2.5_TOTAL] and [4.5_TOTAL] and between [2.5_INTERNAL] and [4.5_INTERNAL] with respect to trueness and precision values.

The orientation of the printed parts on the building platform could be a decisive co-factor influencing accuracy.

A higher volume of printed objects resulted in increased deviations regarding trueness and precision.

Trueness and precision values of the tested digital light processing printer were competitive to the results published for other printers when occlusal devices were evaluated.

Author Contributions: Conceptualization, S.B., H.H. and S.R.; data curation, S.B. and H.H.; investigation, S.B., H.H. and S.R.; methodology, S.B., H.H. and S.R.; project administration, S.R.; supervision, S.R.; visualization, S.B., H.H., S.R. and C.K.; writing—original draft, S.B., H.H. and S.R.; writing—review & editing, S.B., H.H. and S.R. All authors have read and agreed to the published version of the manuscript.

Funding: The research was funded by Dentsply Sirona.

Institutional Review Board Statement: Not applicable.

Informed Consent Statement: Not applicable.

Data Availability Statement: The data presented in this study are available on request from the corresponding author.

Acknowledgments: Thanks to Berfin Yatmaz for giving advice.

Conflicts of Interest: The author S.R. has or had commercial relationships with the following companies including consulting, presentation activities, and third party-funded research: 3M OralCare, 3Shape, Amann Girrbach, Camlog, Oral Reconstruction Foundation, DCS, Dentaurum, Dentsply Sirona, Ivoclar Vivadent, Straumann, Vita Zahnfabrik. S.B., and H.H. declare no conflict of interest.

References

1. Klasser, G.D.; Greene, C.S. Oral appliances in the management of temporomandibular disorders. *Oral Surg. Oral Med. Oral Pathol. Oral Radiol. Endod.* **2009**, *107*, 212–223. [[CrossRef](#)] [[PubMed](#)]
2. Fricton, J.; Look, J.O.; Wright, E.; Alencar, F.G., Jr.; Chen, H.; Lang, M.; Ouyang, W.; Velly, A.M. Systematic review and meta-analysis of randomized controlled trials evaluating intraoral orthopedic appliances for temporomandibular disorders. *J. Orofac. Pain* **2010**, *24*, 237–254. [[PubMed](#)]

3. Proff, P.; Richter, E.J.; Blens, T.; Fanghanel, J.; Hutzen, D.; Kordass, B.; Gedrange, T.; Rottner, K. A michigan-type occlusal splint with spring-loaded mandibular protrusion functionality for treatment of anterior disk dislocation with reduction. *Ann. Anat.* **2007**, *189*, 362–366. [[CrossRef](#)]
4. Schindler, H.J.; Hugger, A.; Kordaß, B.; Türp, J.C. Splint therapy for temporomandibular disorders: Basic principles. *J. Cranio-mandib. Funct.* **2014**, *6*, 207–230.
5. Leib, A.M. The occlusal bite splint—A noninvasive therapy for occlusal habits and temporomandibular disorders. *Compend. Contin. Educ. Dent.* **1996**, *17*, 1081–1084, 1086, 1088. [[PubMed](#)]
6. Turp, J.C.; Komine, F.; Hugger, A. Efficacy of stabilization splints for the management of patients with masticatory muscle pain: A qualitative systematic review. *Clin. Oral Investig.* **2004**, *8*, 179–195. [[CrossRef](#)]
7. Reyes-Sevilla, M.; Kuijs, R.H.; Werner, A.; Kleverlaan, C.J.; Lobbezoo, F. Comparison of wear between occlusal splint materials and resin composite materials. *J. Oral Rehabil.* **2018**, *45*, 539–544. [[CrossRef](#)]
8. Macedo, C.R.; Silva, A.B.; Machado, M.A.; Saconato, H.; Prado, G.F. Occlusal splints for treating sleep bruxism (tooth grinding). *Cochrane Database Syst. Rev.* **2007**, CD005514. [[CrossRef](#)]
9. Edelhoff, D.; Schweiger, J.; Prandtner, O.; Trimpl, J.; Stimmelmayer, M.; Guth, J.F. CAD/CAM splints for the functional and esthetic evaluation of newly defined occlusal dimensions. *Quintessence Int.* **2017**, *48*, 181–191. [[CrossRef](#)]
10. Vayrynen, V.O.; Tanner, J.; Vallittu, P.K. The anisotropy of the flexural properties of an occlusal device material processed by stereolithography. *J. Prosthet. Dent.* **2016**, *116*, 811–817. [[CrossRef](#)]
11. Kass, C.A.; Tregaskes, J.N. Occlusal splint fabrication. *J. Prosthet. Dent.* **1978**, *40*, 461–463. [[CrossRef](#)]
12. Becker, C.M.; Kaiser, D.A.; Lemm, R.B. A simplified technique for fabrication fo night guards. *J. Prosthet. Dent.* **1974**, *32*, 582–589. [[CrossRef](#)]
13. Bohnenkamp, D.M. Dimensional stability of occlusal splints. *J. Prosthet. Dent.* **1996**, *75*, 262–268. [[CrossRef](#)]
14. Grymak, A.; Aarts, J.M.; Ma, S.; Waddell, J.N.; Choi, J.J.E. Wear Behavior of Occlusal Splint Materials Manufactured By Various Methods: A Systematic Review. *J. Prosthodont.* **2021**. [[CrossRef](#)] [[PubMed](#)]
15. Huettig, F.; Kustermann, A.; Kuscu, E.; Geis-Gerstorf, J.; Spintzyk, S. Polishability and wear resistance of splint material for oral appliances produced with conventional, subtractive, and additive manufacturing. *J. Mech. Behav. Biomed. Mater.* **2017**, *75*, 175–179. [[CrossRef](#)] [[PubMed](#)]
16. Reymus, M.; Stawarczyk, B. In vitro study on the influence of postpolymerization and aging on the Martens parameters of 3D-printed occlusal devices. *J. Prosthet. Dent.* **2021**, *125*, 817–823. [[CrossRef](#)]
17. Marcel, R.; Reinhard, H.; Andreas, K. Accuracy of CAD/CAM-fabricated bite splints: Milling vs 3D printing. *Clin. Oral Investig.* **2020**, *24*, 4607–4615. [[CrossRef](#)]
18. Berli, C.; Thieringer, F.M.; Sharma, N.; Muller, J.A.; Dedem, P.; Fischer, J.; Rohr, N. Comparing the mechanical properties of pressed, milled, and 3D-printed resins for occlusal devices. *J. Prosthet. Dent.* **2020**, *124*, 780–786. [[CrossRef](#)]
19. Wesemann, C.; Spies, B.C.; Sterzenbach, G.; Beuer, F.; Kohal, R.; Wemken, G.; Krugel, M.; Pieralli, S. Polymers for conventional, subtractive, and additive manufacturing of occlusal devices differ in hardness and flexural properties but not in wear resistance. *Dent. Mater.* **2021**, *37*, 432–442. [[CrossRef](#)]
20. Kattadiyil, M.T.; Jekki, R.; Goodacre, C.J.; Baba, N.Z. Comparison of treatment outcomes in digital and conventional complete removable dental prosthesis fabrications in a predoctoral setting. *J. Prosthet. Dent.* **2015**, *114*, 818–825. [[CrossRef](#)]
21. Pagac, M.; Hajnys, J.; Ma, Q.P.; Jancar, L.; Jansa, J.; Stefek, P.; Mesicek, J. A Review of Vat Photopolymerization Technology: Materials, Applications, Challenges, and Future Trends of 3D Printing. *Polymers* **2021**, *13*, 598. [[CrossRef](#)]
22. Hui, J.; Ding, K.; Chan, F. An investigation on energy consumption and part quality of stereolithography apparatus manufactured parts. *Rapid Prototyp. J.* **2022**, *28*, 52–67. [[CrossRef](#)]
23. Sim, J.Y.; Jang, Y.; Kim, W.C.; Kim, H.Y.; Lee, D.H.; Kim, J.H. Comparing the accuracy (trueness and precision) of models of fixed dental prostheses fabricated by digital and conventional workflows. *J. Prosthodont. Res.* **2019**, *63*, 25–30. [[CrossRef](#)] [[PubMed](#)]
24. Ligon, S.C.; Liska, R.; Stampfl, J.; Gurr, M.; Mulhaupt, R. Polymers for 3D Printing and Customized Additive Manufacturing. *Chem. Rev.* **2017**, *117*, 10212–10290. [[CrossRef](#)]
25. Alifui-Segbaya, F. Biomedical photopolymers in 3D printing. *Rapid Prototyp. J.* **2019**, *26*, 437–444. [[CrossRef](#)]
26. Revilla-Leon, M.; Ozcan, M. Additive Manufacturing Technologies Used for Processing Polymers: Current Status and Potential Application in Prosthetic Dentistry. *J. Prosthodont.* **2019**, *28*, 146–158. [[CrossRef](#)]
27. Kumar, M.V. Additive manufacturing techniques for the fabrication of tissue engineering scaffolds: A review. *Rapid Prototyp. J.* **2021**, *27*, 1230–1272. [[CrossRef](#)]
28. Etemad-Shahidi, Y.; Qallandar, O.B.; Evenden, J.; Alifui-Segbaya, F.; Ahmed, K.E. Accuracy of 3-Dimensionally Printed Full-Arch Dental Models: A Systematic Review. *J. Clin. Med.* **2020**, *9*, 3357. [[CrossRef](#)]
29. Tumbleston, J.R.; Shrivanyants, D.; Ermoshkin, N.; Januszewicz, R.; Johnson, A.R.; Kelly, D.; Chen, K.; Pinschmidt, R.; Rolland, J.P.; Ermoshkin, A.; et al. Additive manufacturing. Continuous liquid interface production of 3D objects. *Science* **2015**, *347*, 1349–1352. [[CrossRef](#)]
30. Balkenhol, M. *Dentale CAD/CAM-Technologie Thieme*; Thieme Verlag: Stuttgart, Germany, 2018.
31. Stansbury, J.W.; Idacavage, M.J. 3D printing with polymers: Challenges among expanding options and opportunities. *Dent. Mater.* **2016**, *32*, 54–64. [[CrossRef](#)]

32. Methani, M.M.; Revilla-Leon, M.; Zandinejad, A. The potential of additive manufacturing technologies and their processing parameters for the fabrication of all-ceramic crowns: A review. *J. Esthet. Restor. Dent.* **2019**, *32*, 182–192. [[CrossRef](#)] [[PubMed](#)]
33. Pillai, S.; Upadhyay, A.; Khayambashi, P.; Farooq, I.; Sabri, H.; Tarar, M.; Lee, K.T.; Harb, I.; Zhou, S.; Wang, Y.; et al. Dental 3D-Printing: Transferring Art from the Laboratories to the Clinics. *Polymers* **2021**, *13*, 157. [[CrossRef](#)] [[PubMed](#)]
34. Schlotthauer, T.; Nitsche, J.; Middendorf, P. Evaluation of UV post-curing depth for homogenous cross-linking of stereolithographic parts. *Rapid Prototyp. J.* **2021**, *27*, 1910–1916. [[CrossRef](#)]
35. Unkovskiy, A.; Bui, P.H.; Schille, C.; Geis-Gerstorfer, J.; Huettig, F.; Spintzyk, S. Objects build orientation, positioning, and curing influence dimensional accuracy and flexural properties of stereolithographically printed resin. *Dent. Mater.* **2018**, *34*, e324–e333. [[CrossRef](#)] [[PubMed](#)]
36. Kim, N.; Bhalerao, I.; Han, D.; Yang, C.; Lee, H. Improving Surface Roughness of Additively Manufactured Parts Using a Photopolymerization Model and Multi-Objective Particle Swarm Optimization. *Appl. Sci.* **2019**, *9*, 151. [[CrossRef](#)]
37. Wu, X.; Xu, C.; Zhang, Z.; Jin, Z. Tilting separation simulation and theory verification of mask projection stereolithography process. *Rapid Prototyp. J.* **2021**, *27*, 851–860. [[CrossRef](#)]
38. Mehl, A.; Reich, S.; Beuer, F.; Güth, J. Accuracy, trueness, and precision—A guideline for evaluation of these basic values in digital dentistry. *Int. J. Comput. Dent.* (in press). **2021**, *24*, 1–11.
39. International Organization for Standardization. *ISO 5725-1. Accuracy (Trueness and Precision) of Measuring Methods and Results. Part-1: General Principles and Definitions*; Beuth Verlag: Berlin, Germany, 1994.
40. Passos, L.; Meiga, S.; Brigagao, V.; Street, A. Impact of different scanning strategies on the accuracy of two current intraoral scanning systems in complete-arch impressions: An in vitro study. *Int. J. Comput. Dent.* **2019**, *22*, 307–319.
41. Dold, P.; Bone, M.C.; Flohr, M.; Preuss, R.; Joyce, T.J.; Deehan, D.; Holland, J. Validation of an optical system to measure acetabular shell deformation in cadavers. *Proc. Inst. Mech. Eng. H* **2014**, *228*, 781–786. [[CrossRef](#)]
42. Wesemann, C.; Spies, B.C.; Schaefer, D.; Adali, U.; Beuer, F.; Pieralli, S. Accuracy and its impact on fit of injection molded, milled and additively manufactured occlusal splints. *J. Mech. Behav. Biomed. Mater.* **2021**, *114*, 104179. [[CrossRef](#)]
43. Yoon, H.I.; Hwang, H.J.; Ohkubo, C.; Han, J.S.; Park, E.J. Evaluation of the trueness and tissue surface adaptation of CAD-CAM mandibular denture bases manufactured using digital light processing. *J. Prosthet. Dent.* **2018**, *120*, 919–926. [[CrossRef](#)] [[PubMed](#)]
44. Wenbin, H.; Tsui, L.; Haiging, G. A study of the staircase effect induced by material shrinkage in rapid prototyping. *Rapid Prototyp. J.* **2005**, *11*, 82–89. [[CrossRef](#)]
45. Park, J.M.; Jeon, J.; Koak, J.Y.; Kim, S.K.; Heo, S.J. Dimensional accuracy and surface characteristics of 3D-printed dental casts. *J. Prosthet. Dent.* **2021**, *126*, 427–437. [[CrossRef](#)] [[PubMed](#)]
46. Bugada, G.; Cervera, M.; Lombera, G.; Onate, E. Numerical analysis of stereolithography processes using the finite element method. *Rapid Prototyp. J.* **1995**, *1*, 13–23. [[CrossRef](#)]